

Machine learning can guide experimental approaches for protein digestibility estimations

Sara Malvar^{1*}, Anvita Bhagavathula², Maria Angels de Luis Balaguer¹, Swati Sharma¹ and Ranveer Chandra¹

^{1*}Microsoft Research, Microsoft Building 99, 15010 NE 36th St 2, Redmond, 09805, Wa, USA.

²Brown University, Providence, 02912, RI, USA.

*Corresponding author(s). E-mail(s): saramalvar@microsoft.com;

Abstract

Food protein digestibility and bioavailability are critical aspects in addressing human nutritional demands, particularly when seeking sustainable alternatives to animal-based proteins. In this study, we propose a machine learning approach to predict the true ileal digestibility coefficient of food items. The model makes use of a unique curated dataset that combines nutritional information from different foods with FASTA sequences of some of their protein families. We extracted the biochemical properties of the proteins and combined these properties with embeddings from a Transformer-based protein Language Model (pLM). In addition, we used SHAP to identify features that contribute most to the model prediction and provide interpretability. This first AI-based model for predicting food protein digestibility has an accuracy of 90% compared to existing experimental techniques. With this accuracy, our model can eliminate the need for lengthy *in-vivo* or *in-vitro* experiments, making the process of creating new foods faster, cheaper, and more ethical.

Keywords: DIAAS, protein digestibility, AI, ML interpretability

1 Introduction

The increase in the world population and the need for more nutritious food will increase the demand for animal-based foods by nearly 70%, particularly from ruminant meat [1]. Closing this food gap will intensify the pressure on land usage and contribute to an increase in greenhouse gas (GHG) emissions [2]. Due to such environmental concerns, transitioning towards more sustainable diets and exploring alternative protein sources have been at the forefront of 21st century research [3].

Although plant proteins have already been associated with lowering the risk of type 2 diabetes, cardiovascular diseases, hypertension, obesity, metabolic syndrome and all-cause mortality in prospective cohort studies [4–7], there is still a long way to go in terms of texture, flavor, and bioavailability. A common concern among consumers is recognizing which foods are good protein sources and whether proteins from plants are of as good quality as those from animal-derived foods. The interaction between animal and plant proteins is being comprehensively investigated to develop balanced mixtures of animal and vegetable proteins. These studies involve determining and understanding protein structure-function relations, optimizing the use of the components of the product, improving the quality, reducing costs, and finding new protein applications.

Protein quality is defined by the essential amino acid composition of the protein, as well as the bioavailability and digestibility of its constituent amino acids. Over the last few decades, tremendous effort has been made to develop methodologies for measuring protein quality. The Food and Agriculture Organization of the United Nations (FAO) currently advises evaluating protein quality in human diets using Digestible Indispensable Amino Acid Score (DIAAS) values, which are measured through human or pig ileal digesta [8]. Unlike older methods such as Protein Digestibility Corrected Amino Acid Score (PDCAAS) values, DIAAS values are obtained by multiplying the digestibility of each essential AA by its concentration in the protein and then comparing the results to a scoring system [9]. This digestion process can also be simulated *in-vitro*. In this case, the digestibility is measured by monitoring the amount of soluble proteins, changes in digesta pH (reflecting protein hydrolysis), or the level of increase in the nitrogen not incorporated in protein structures (i.e., nonprotein nitrogen) [10]. Although *in-vitro* analysis can be cheaper and easier than the methods to predict the outcome of *in-vivo* digestibility, the complexity of *in-vivo* digestibility has not been realized fully in an *in-vitro* model [11]. In addition, working with animals can be time consuming, costly and one could face ethical barriers.

Currently, an important goal for food manufacturers is to replicate the flavor profiles, texture, and bioavailability of a meat replacement. This approach has traditionally been quite repetitious, with hundreds of alternative protein source formulations eventually narrowed down to the most comparable profile. In this work, we aim to provide a solution to accelerate this process at a

reduced cost through the use of an AI model for protein digestibility prediction. Our contributions are as follows:

1. **Dataset creation** We combine nutritional information such as dietary fiber content, fat, and vitamins of various foods with the FASTA sequences of their protein families. We use these sequences for a feature extraction step that aims to identify protein structural characteristics. The extracted structural features and the nutritional information formed the basis of our dataset used to predict the DIAAS value. The feature vector for each food consists of their structural and nutritional characteristics, amino acid composition and some categorical variables related to the food type. To our knowledge, this is the first attempt to associate these disparate features and use them in a machine learning (ML) model.
2. **Interpretability** We select the features with higher predictive power, and, consequently, facilitate the model's interpretability. Selecting these features enhanced the model's performance due to dimensionality reduction. Exploring model interpretability is an important step to guide new experiments and new food design processes, as it gives insight on how protein engineering can be used to change protein's structural information to increase a food's digestibility. Similarly, it can guide how we can add/remove salts, decrease dietary fiber content and manipulate the nutritional information to achieve higher bioavailability. In addition to that, we were able to confirm some important proved correlations between food nutrients and protein digestibility.
3. **ML modeling** We developed an alternative ML-based approach to predict the DIAAS score that avoids *in-vivo* and *in-vitro* testing, is cost-effective, and fast. With a 90% accuracy compared to experimental approaches, our model can be used to guide experimental approaches by testing new protein sources in a faster, cheaper, and ethical manner. Our ML model targets true ileal digestibility coefficient of each indispensable amino acid, which allows us to calculate DIAAS for each food item, considering the reference values.

2 Results

2.1 Dataset curation

To be able to train a model that can predict digestibility, it is necessary to obtain training data. To our knowledge, there was no public ground truth data available at this point, especially for DIAAS, as it has been proposed more recently. Thus, a complete database was developed for this analysis using the following original data:

- First, a database containing ileal amino acid digestibility values for more than 180 food items along with the associated DIAAS values in cases where adequate information was reported to derive this score [12] was used. This data was obtained from over 30 references presented in supplementary table 2. This feature is defined as our target variable.

- Nutritional information for foods such as fat, potassium and sodium content was obtained from data from the FoodData Central of the United States Department of Agriculture (USDA) [13] and Food Data from the National Food Institute in the Technical University of Denmark [14]. For each food item in the database, the features presented in supplementary tables 3 and 4 were also added.
- In order to capture additional protein features, the FASTA sequence of at least two of the most abundant proteins from different protein families of each food item were added to the dataset. Then, their physio-chemical and biochemical properties were generated using Protlearn [15] and added to the database. These features are shown in section 5.8 of the Supplementary Material.

2.2 Baseline models

First, 12 baseline regressors were trained on all 1671 features of 189 food items. The R^2 values and RMSE of the 12 models is shown in section 5.4 of the Supplementary Material. The 3 top-performing models were based on boosting and bagging techniques applied to decision trees: LightGBM, XGBoost and Random Forest. The target variable was defined as the true ileal digestibility coefficient of each indispensable amino acid, as further detailed in Methods. As reported in section 5.4 of the Supplementary Material, we found that the Random Forest, XGBoost, and LightGBM models predicted the ileal digestibility coefficient with a validation R^2 of 0.83, 0.87, and 0.88 respectively.

2.3 Feature selection and SHAP values

The second step of many ML methods is the feature extraction, the aim of which is to get the most effective features from the obtained raw segment. This problem was approached as a feature selection or dimensionality reduction method, which is pervasive in all domains of application of machine learning and data mining. To understand the importance of the features in the model and provide some explainability, a sensitivity based method called SHAP [16] was used for feature importance evaluation [17] (see Methods). First, we determined the importance of the features using SHAP. Then, we used Principal Component Analysis [18] and determined that the top 20 features explained above 95% of the model variance. Therefore, we selected these features for our model, as shown in figure 1. The color represents the feature value, where red indicates high and blue indicates low. It is noticeable that some of the SHAP-selected features presented as important are known in the literature for their direct effect on digestibility. For instance, Mongeau [19] shows that the true protein digestibility in rats was negatively correlated with the total food fiber level. Likewise, the type of limiting amino acid is directly associated with the true ileal digestibility of that amino acid. Salts like magnesium and manganese are also associated with a lower rate of protein digestibility, disrupting the enzymatic process [20, 21].

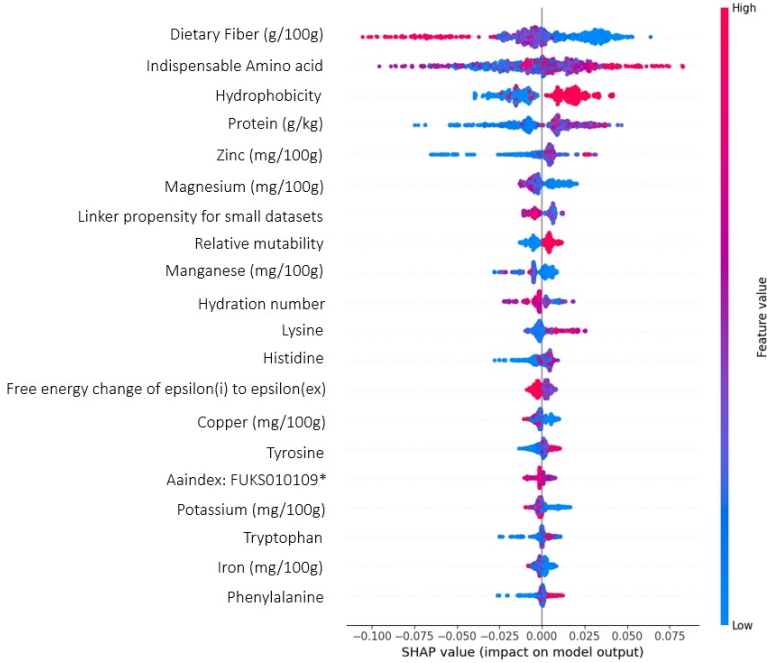


Fig. 1 The local explanation summary of the model represents a set of beeswarm plots, where each dot corresponds to an individual sample in the study. The dot's position on the x axis shows the impact that feature has on the model's prediction for that person. When multiple dots land at the same x position, they pile up to show density.

Protein digestibility is also found to be positively correlated with surface hydrophobicity of proteins through a study on heat-induced protein unfolding [22]. Hydrophobic groups are normally buried within protein structure. However, the unfolding of proteins exposes hydrophobic residues to the surface, increasing overall surface hydrophobicity and providing easier access for digestive enzymes to hydrolyze the protein [22]. Our model found other features associated with surface hydrophobicity, such as hydration number and linker propensity, to also confirm this correlation. For example, the hydration number indicates how likely a water molecule is to bind to a solute as compared to other water molecules [23], implying that the hydration number is inversely linked to hydrophobicity and therefore to protein digestibility too [24]. Similarly, linker propensity, or a tendency of a protein to have high numbers of linkers, can be linked to hydrophilicity since preferred linker amino acids have been established to be mostly hydrophilic [24].

Several minerals have also been shown to impact digestibility in accordance with our Shapley value results. For instance, Pallauf and Kirchgessner demonstrate that zinc deficiency has a negative effect on nutrient digestibility in weaned male rats [25]. Salts containing potassium, such as Potassium thiocyanate, were shown to be trypsin inhibitors, which are in turn known to reduce the digestion and absorption of dietary proteins [26] [27]. Additionally,

specific amino acids have been established as having an impact on protein digestibility. Amino acids such as lysine and histidine have been demonstrated to have a positive impact on food intake and metabolism [28] [29]. For example, L-lysine delayed intestinal transit in rats [28], potentially increasing ileal protein absorption by increasing the time the protein resided in the small intestine [30]. Other amino acids, such as Tryptophan and phenylalanine, have been shown to modulate gut microbiota and the secretion of digestive enzymes [31] [32], likely increasing the amount of protein absorption.

2.4 Protein embeddings from language model

It is known that protein structure helps in understanding function. To be able to understand how the structure of proteins modify the digestibility of proteins, we used a language model approach. Here, we assume that the protein sequence is a series of tokens, or characters, such as a text corpus. Protein sequences are inherently similar to natural languages: amino acids arrange in a multitude of combinations to form structures that carry function, the same way as letters form words and sentences, which carry meaning [33].

To make the model more robust, we extracted embeddings from the protein sequences using ProtTrans, a language model trained with UniRef50 and BFD100 [34] and added these embeddings to the final dataset. The final architecture of our method is shown in figure 2.

2.5 Model results

When creating this unique machine learning model, we used several concepts that contribute to the overall model performance. In the ablation study, we try to identify the influence of each of these innovations separately. Details of the ablation study can be found on section 5.6 of the Supplementary Material.

The results of the ablation study are shown in table 1, which shows the R^2 of each model. We see that the SHAP method performed better than solely using feature importance from the LGBM model. Additionally, adding the ProtTrans embeddings also increases the model's R^2 . The R^2 of the final model is shown in figure 3. The sensitivity analysis done for each group of variables is also shown in section 5.7 of the Supplementary Material.

Model	Description	R^2
Model A	Baseline LGBM	0.87730
Model B	After LGBM feature importance selection	0.89256
Model C	After LGBM feature importance selection + transformer embeddings	0.90003
Model D	After SHAP selection	0.89901
Model E	After SHAP selection + transformer embeddings	0.90165

Table 1 R^2 of the models trained on the ablation study.

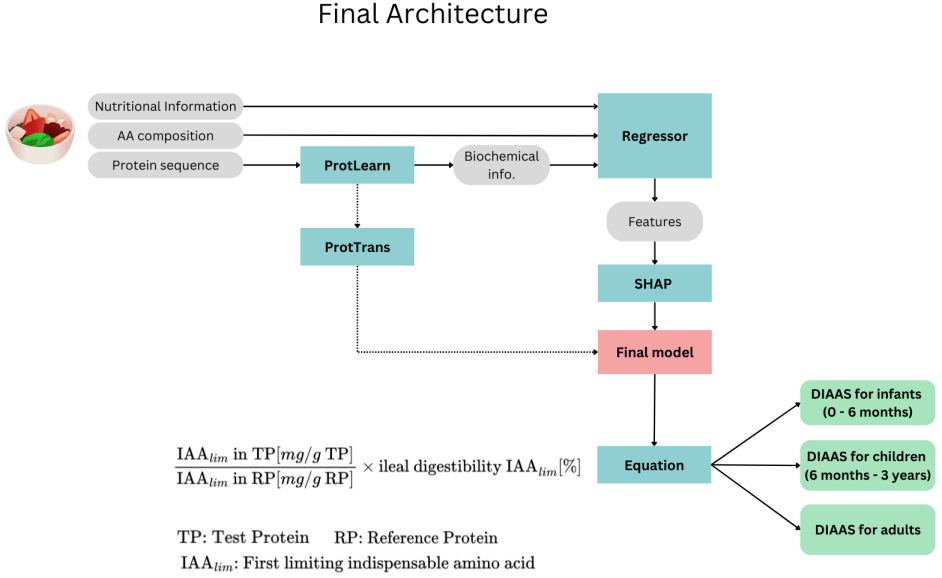


Fig. 2 Final architecture of the proposed method. For each food item, nutritional information, amino acid composition and protein sequences of at least two families are required. The algorithm includes two feature extraction steps: biochemical information is extracted using Protlearn [15] and embeddings are extracted using ProtT5 [34]. The baseline regressors are trained and two feature selection approaches are compared: feature importance from LGBM and SHAP [16]. The true ileal digestibility for each indispensable amino acid and food item is predicted and the DIAAS value is calculated for three different categories: infants, children and adults.

3 Discussion

We propose an approach that allows us to predict the true ileal digestibility coefficient for each indispensable amino acid in a food, a value normally determined experimentally using *in-vivo* or *in-vitro* methods. Our data-science based method enabled us to estimate this value with 90% R^2 accuracy. Not only is our proposed method novel in approximating the ileal digestibility coefficient of foods, as it is solely computational, but is also able to capture established relationships through its features and model output. Additionally, there are many potential downstream applications of our approach.

For instance, the approach itself can help accelerate the production of alternative protein products. Food scientists can use this approach to evaluate a large number of promising target proteins computationally and decrease the size of their experimental matrices. This methodology can also help predicting DIAAS for complex food matrices or for scenarios where *in-vivo* and *in-vitro* options cannot be used. In addition to the potential to streamline experimentation, our methodology's interpretability could incite scientists to propose new scientific experiments to better understand how protein structure is related

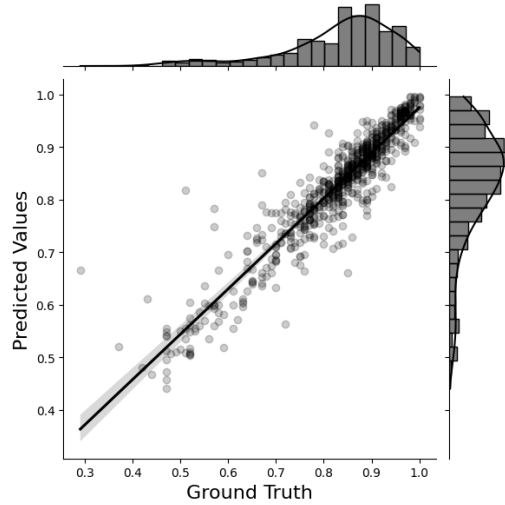


Fig. 3 The R^2 of the model can be visually represented by the trend analysis of the ground truth data plotted against the predicted values. For each data point the values should be similar. Besides a few outliers, both ground truth and predicted distributions are similar.

to digestibility. We were able to capture some of these structure-activity relationships using the 20 most important features generated by Shapley value analysis. Our model's interpretability could guide *in-vivo* experiments to better identify the direct relationship of these other variables with digestibility, reducing the array of possible experimental combinations when investigating these relationships. As new primary data is collected and becomes available, it is important perform regular re-trainings on our model to improve its explanatory power.

This highlights one of the fundamental challenges of our approach and the basis for our future research: the size of our curated dataset. As more data becomes available, we can retrain the model to capture less frequent patterns that are specific to local contexts, foods, and proteins. ML techniques often do not make assumptions on the exact functional form of the model and attempt to learn the model form directly from the data, such that it maximizes prediction accuracy. To do so, they take into account linear and non-linear correlations between the data, but do not take into account cause and effect relationships. In this situation, this means that the model learns patterns in the data based on the most commonly observed relationships across protein families. Therefore, with a dataset with items ranging from processed foods to raw foods and meat analogues to animal products, more variability would be added and a generalizable model can be obtained.

Much of the ground truth data used in this study was experimentally determined using the grown pig model, which is a valid animal model for this purpose [35, 36]. However, it has been established that food particle size

impacts ileal digestibility values in pigs, with a decrease in particle size increasing apparent ileal digestibility [37]. This might introduce variance into the model, as the ileal digestibility values in our dataset were obtained from different experiments; there is likely limited consistency in food particle size across these experiments.

Another avenue for future research is to add features related to food processing. For instance, it is known that heat treatments applied to food can alter AA digestibility and bioavailability levels when compared to the same, untreated food [38–41]. Other values which we have not featurized are antinutritional factors, whose presence are known to decrease protein digestibility. For instance, tannins or polyphenols produce denaturation of proteins, and protease inhibitors can inhibit trypsin, pepsin, and other proteases in the gut, preventing digestion and absorption of proteins and amino acids. The dataset also fails to consider farming practices, which also affect the protein content of plants and livestock. For example, fertilization regimes can promote nutrients transfer to grains and changes in protein content [42, 43]. Animal husbandry and nutrition also impact growth, productivity and protein content of animal products [44–46].

Overall, our model could be enriched with features that represent a food’s structural information, antinutrients, processing, and the farming practices employed when it was growing. However, obtaining these data for a large number of food items is challenging. This demonstrates the strong need for a unified database that contains such information, more experiments to create ground truth values, and the need to iterate over our existing methodology to make it more robust once new data becomes available. In the meantime, using this purely computational, ethical, and affordable model can enable scientists to reduce the size of their experimental food matrices during protein digestibility experiments, especially in the development of new foods.

4 Methods

4.1 Dataset creation details

The final dataset obtained was created using the original 300 food items present on Muleya and Salter dataset [12]. In cases where digestibility information was missing for some amino acids, an average value based on the reported amino acid data was assigned - average values are indicated in the dataset. Total amino acid and protein composition was obtained from the same source. Values were expressed in g/kg and recalculation was done in cases where the units reported in the reference were different. Digestible indispensable amino acids were calculated by multiplying the digestibility coefficient with the corresponding indispensable amino acid composition expressed in g/kg. Finally, digestible indispensable amino acids were expressed as mg/g protein by dividing the digestible indispensable amino acid composition with the total protein and converting to mg. DIAAS values were calculated for all age groups using

the FAO recommended reference patterns. DIAAS values for some foods are missing due to insufficient information being reported in some cases.

The nutritional information for foods was obtained from the FoodData Central of the United States Department of Agriculture (USDA) [13]. FoodData Central is an integrated data system that provides expanded nutrient profile data and links to related agricultural and experimental research. For each food item in the database, the features presented in tables 3 and 4 were added.

In order to capture additional protein features, their physio-chemical and biochemical properties were added to the database. For this, the amino acid FASTA sequence for each protein was first collected from UniProt [47] or from the NCBI [48] protein database. For this, we selected up to three protein families of the food items, such as albumins, caseins and globulins, when present and Protlearn v2.1 [15] was then used to extract the features from the FASTA sequences. This led to a total of 1671 features that were added to the database for each protein. All features obtained from Protlearn are present in section 5.8 of the Supplementary Material.

Finally, the language model was used to obtain the embeddings of each protein family. The cleaned dataset was composed of almost 200 food items.

4.2 Baseline modeling approach

First, baseline regressors on all 1671 features of 189 food items were trained. The first 3 top-performing models were based on boosting and bagging techniques of decision trees. These models are also able to deal with high-dimensional data that may contain non-linear effects and many interactions between covariates, and can be used to rank the most important predictors to gain insight into the resulting prediction model. Hyperparameters of these three models were optimized using a combination of a randomized grid search technique and manual tuning using stratified 5-fold cross-validation on the training set. Using the optimized tree-based models, the validation R^2 accuracy was calculated on a held-out test set.

4.3 SHAP

Interpretability of models in AI is central to the practical impact of AI on society. Thus it can be treated as a problem of attribution. Shapley values [49] provide the unique attribution method satisfying a set of intuitive axioms, e.g. they capture all interactions between features and sum to the model prediction. Given our baseline predictive model, SHAP yields a vector of importance scores associated with the underlying features. The Shapley value was first introduced as an axiomatic characterisation of a fair distribution of a total surplus from all players, and it may be used in predictive models where each feature is treated as a participant in the underlying game. While the Shapley value technique is conceptually appealing, it is also computationally demanding: in general, each Shapley value assessment demands an exponential number of model evaluations.

Classic Shapley values calculated through SHAP can be considered optimal since, within a large class of approaches, they are the only way to measure feature importance while maintaining several natural properties from cooperative game theory [50]. Shapley also observes the value as an index for assessing the power of participants in a game, in addition to a model that seeks to predict the distribution of resources in multi-feature interactions. The value, like a price index or other market indices, aggregates the strength of actors in their numerous cooperation opportunities using averages (or weighted averages in certain extensions). The Shapley value may also be thought of as a measure of the utility of players/features in a game/model. Several studies have used Shapley values and SHAP package to improve the interpretability of tree-based models [50, 51].

4.4 ProtTrans

The goal of language modelling is to estimate the probability distribution of various linguistic units, e.g., words, sentences. After training the language model (LM), we can extract some information learned by the LMs, referred to as embeddings. This process indicates that when a language model better understands the sequence, it also better understands the structure.

Protein Language Models (pLMs) copy the concepts of Language Models from NLP by using tokens (words in NLP), i.e., amino acids from protein sequences, and treating entire proteins like sentences in LMs. In step 1, these pLMs are trained in a self-supervised manner, essentially learning to predict masked amino acids (tokens) in already known sequences.

ProtTrans [34] is a 3B-parameter model that has an encoder and decoder architecture and allows us to extract 1024 embeddings for each protein sequence using the 1B-parameter encoder. Thus, 1024 embeddings were generated for each of the three protein families of each food item.

References

- [1] World Bank. *World Development Report 2008: Agriculture for Development* (The World Bank, 2007).
- [2] Henchion, M., Hayes, M., Mullen, A., Fenelon, M. & Tiwari, B. Future Protein Supply and Demand: Strategies and Factors Influencing a Sustainable Equilibrium. *Foods* **6**, 53 (2017).
- [3] Nadathur, S. R., Wanasundara, J. P. D. & Scanlin, L. *Sustainable protein sources* (Academic Press in an imprint of Elsevier, Amsterdam, 2017).
- [4] Yokoyama, Y. *et al.* Vegetarian Diets and Blood Pressure: A Meta-analysis. *JAMA Internal Medicine* **174**, 577 (2014).
- [5] Satija, A. *et al.* Plant-Based Dietary Patterns and Incidence of Type 2 Diabetes in US Men and Women: Results from Three Prospective Cohort

- Studies. *PLOS Medicine* **13**, e1002039 (2016).
- [6] Dinu, M., Abbate, R., Gensini, G. F., Casini, A. & Sofi, F. Vegetarian, vegan diets and multiple health outcomes: A systematic review with meta-analysis of observational studies. *Critical Reviews in Food Science and Nutrition* **57**, 3640–3649 (2017).
 - [7] Kim, H. *et al.* Plant-Based Diets Are Associated With a Lower Risk of Incident Cardiovascular Disease, Cardiovascular Disease Mortality, and All-Cause Mortality in a General Population of Middle-Aged Adults. *Journal of the American Heart Association* **8**, e012865 (2019).
 - [8] FAO. Dietary protein quality evaluation in human nutrition. Report of an FAQ Expert Consultation. *FAO food and nutrition paper* **92**, 1–66 (2013).
 - [9] Rutherfurd, S. M., Fanning, A. C., Miller, B. J. & Moughan, P. J. Protein digestibility-corrected amino acid scores and digestible indispensable amino acid scores differentially describe protein quality in growing male rats. *The Journal of Nutrition* **145**, 372–379 (2015).
 - [10] Kårlund, A. *et al.* Harnessing Microbes for Sustainable Development: Food Fermentation as a Tool for Improving the Nutritional Quality of Alternative Protein Sources. *Nutrients* **12**, E1020 (2020).
 - [11] Bohn, T. *et al.* Correlation between in vitro and in vivo data on food digestion. What can we predict with static in vitro digestion models? *Critical Reviews in Food Science and Nutrition* **58**, 2239–2261 (2018).
 - [12] Muleya, M. & Salter, A. Ileal amino acid digestibility and DIAAS values of world foods (2021). <https://data.mendeley.com/datasets/gz3cx7d5f4/1>.
 - [13] US Department of Agriculture (USDA), N. D., Agricultural Research Service. USDA National Nutrient Database for Standard Reference, Legacy. <http://www.ars.usda.gov/nutrientdata>.
 - [14] National Food Institute, T. U. o. D. Fooda data. <https://frida.fooddata.dk/?lang=en>.
 - [15] Dorfer, T. Protlearn Package. <https://github.com/tadorfer/protlearn>.
 - [16] Guyon, I. *et al.* Advances in Neural Information Processing Systems. In *30: Annual Conference on Neural Information Processing System* (Long Beach, CA, USA, 2017).

- [17] Lundberg, S. & Lee, S.-I. A Unified Approach to Interpreting Model Predictions (2017). URL <http://arxiv.org/abs/1705.07874>. ArXiv:1705.07874 [cs, stat].
- [18] Jolliffe, I. T. *Principal Component Analysis*. Springer Series in Statistics (Springer-Verlag, New York, 2002). URL <http://link.springer.com/10.1007/b98835>.
- [19] Mongeau, R., Sarwar, G., Peace, R. W. & Brassard, R. Relationship between dietary fiber levels and protein digestibility in selected foods as determined in rats. *Plant Foods for Human Nutrition (Dordrecht, Netherlands)* **39**, 45–51 (1989).
- [20] Kaspchak, E., Goedert, A. C., Igarashi-Mafra, L. & Mafra, M. R. Effect of divalent cations on bovine serum albumin (BSA) and tannic acid interaction and its influence on turbidity and in vitro protein digestibility. *International Journal of Biological Macromolecules* **136**, 486–492 (2019).
- [21] Geboes, K. P. *et al.* Magnesium chloride slows gastric emptying, but does not affect digestive functions. *Aliment Pharmacol Ther* **16**, 1571–1577 (2002).
- [22] Tang, J., Wichers, H. J. & Hettinga, K. A. Heat-induced unfolding facilitates plant protein digestibility during in vitro static infant digestion. *Food Chemistry* **375**, 131878 (2022).
- [23] Zavitsas, A. A. Some opinions of an innocent bystander regarding the Hofmeister series. *Current Opinion in Colloid & Interface Science* **23**, 72–81 (2016).
- [24] Sagawa, N. & Shikata, T. Are all polar molecules hydrophilic? Hydration numbers of nitro compounds and nitriles in aqueous solution. *Physical chemistry chemical physics* **16**, 13262–13270 (2014).
- [25] Pallauf, J. & Kirchgessner, M. Einfluß mangelnder Zinkversorgung auf Verdaulichkeit und Verwertung von Nährstoffen. *Archiv für Tierernährung* **26**, 457–473 (1976).
- [26] Shikimi, T., Kobayashi, T. & Hattori, K. Modes of inhibition of activities of trypsin and chymotrypsin by potassium thiocyanate. *Enzyme* **24**, 348–352 (1979).
- [27] Avilés-Gaxiola, S., Chuck-Hernández, C. & Serna Saldívar, S. O. Inactivation Methods of Trypsin Inhibitor in Legumes: A Review. *Journal of Food Science* **83**, 17–29 (2018).

- [28] Baruffol, C. *et al.* L-lysine dose dependently delays gastric emptying and increases intestinal fluid volume in humans and rats. *Neurogastroenterology & Motility* **26**, 999–1009 (2014).
- [29] Moro, J., Tomé, D., Schmidely, P., Demersay, T.-C. & Azzout-Marniche, D. Histidine: A Systematic Review on Metabolism and Physiological Effects in Human and Different Animal Species. *Nutrients* **12**, E1414 (2020).
- [30] Zhao, X. T., Miller, R. H., McCamish, M. A., Wang, L. & Lin, H. C. Protein absorption depends on load-dependent inhibition of intestinal transit in dogs. *The American Journal of Clinical Nutrition* **64**, 319–323 (1996).
- [31] Taleb, S. Tryptophan Dietary Impacts Gut Barrier and Metabolic Diseases. *Frontiers in Immunology* **10**, 2113 (2019).
- [32] Guo, L. *et al.* Phenylalanine regulates initiation of digestive enzyme mRNA translation in pancreatic acinar cells and tissue segments in dairy calves. *Bioscience Reports* **38**, BSR20171189 (2018).
- [33] Ferruz, N. & Höcker, B. Controllable protein design with language models. *Nature Machine Intelligence* **4**, 521–532 (2022).
- [34] ProtTrans: Toward Understanding the Language of Life Through Self-Supervised Learning **44**, 7112–7127 (2022).
- [35] Moughan, P. J., Birtles, M. J., Cranwell, P. D., Smith, W. C. & Pedraza, M. The piglet as a model animal for studying aspects of digestion and absorption in milk-fed human infants. *World Review of Nutrition and Dietetics* **67**, 40–113 (1992).
- [36] Deglaire, A. & Moughan, P. J. Animal models for determining amino acid digestibility in humans - a review. *The British Journal of Nutrition* **108 Suppl 2**, S273–281 (2012).
- [37] Flis, M., Sobotka, W. & Purwin, C. Effect of feed structure on nutrient digestibility, growth performance, and gastrointestinal tract of pigs – A Review. *Annals of Animal Science* **14**, 757–768 (2014).
- [38] Hodgkinson, S. M., Stein, H. H., de Vries, S., Hendriks, W. H. & Moughan, P. J. Determination of True Ileal Amino Acid Digestibility in the Growing Pig for Calculation of Digestible Indispensable Amino Acid Score (DIAAS). *The Journal of Nutrition* **150**, 2621–2623 (2020).
- [39] Rutherfurd, S. M. & Moughan, P. J. Application of a New Method for Determining Digestible Reactive Lysine to Variably Heated Protein

- Sources. *Journal of Agricultural and Food Chemistry* **45**, 1582–1586 (1997).
- [40] Almeida, F. N., Htoo, J. K., Thomson, J. & Stein, H. H. Amino acid digestibility of heat damaged distillers dried grains with solubles fed to pigs. *Journal of Animal Science and Biotechnology* **4**, 44 (2013).
 - [41] Sá, A. G. A., Moreno, Y. M. F. & Carciofi, B. A. M. Food processing for the improvement of plant proteins digestibility. *Critical Reviews in Food Science and Nutrition* **60**, 3367–3386 (2020).
 - [42] Preet, K. & Punia, D. Antinutrients and digestibility (in vitro) of soaked, dehulled and germinated cowpeas. *Nutrition and Health* **14**, 109–117 (2000).
 - [43] Yan, S. *et al.* Quantifying grain yield, protein, nutrient uptake and utilization of winter wheat under various drip fertigation regimes. *Agricultural Water Management* **261**, 107380 (2022).
 - [44] Zhang, J. *et al.* Effect of Different Tannin Sources on Nutrient Intake, Digestibility, Performance, Nitrogen Utilization, and Blood Parameters in Dairy Cows. *Animals : an Open Access Journal from MDPI* **9**, 507 (2019).
 - [45] Coulon, J. B. & Rémond, B. Variations in milk output and milk protein content in response to the level of energy supply to the dairy cow: A review. *Livestock Production Science* **29**, 31–47 (1991).
 - [46] Tyasi, T., Gxasheka, M. & Tlabela, C. Assessing the effect of nutrition on milk composition of dairy cows: A review. *International Journal of Current Science* 56–63 (2015).
 - [47] Bateman, A. *et al.* UniProt: the universal protein knowledgebase in 2021. *Nucleic Acids Research* **49**, D480–D489 (2021).
 - [48] NCBI. National Center for Biotechnology Information (NCBI). <https://www.ncbi.nlm.nih.gov/>.
 - [49] Shapley, L. S. 17. A Value for n-Person Games. In Kuhn, H. W. & Tucker, A. W. (eds.) *Contributions to the Theory of Games (AM-28), Volume II*, 307–318 (Princeton University Press, 1953).
 - [50] Lundberg, S. M. *et al.* From Local Explanations to Global Understanding with Explainable AI for Trees. *Nature machine intelligence* **2**, 56–67 (2020).

- [51] Lundberg, S. M. *et al.* Explainable machine-learning predictions for the prevention of hypoxaemia during surgery. *Nature Biomedical Engineering* **2**, 749–760 (2018).
- [52] FAO. *FAO Nutritional Studies No. 16. Protein Requirements* (FAO, Rome, 1967).
- [53] EFSA. Scientific Opinion on Dietary Reference Values for protein. *EFSA Journal* (2012).
- [54] Trommelen, J., Tomé, D. & van Loon, L. J. Gut amino acid absorption in humans: Concepts and relevance for postprandial metabolism. *Clinical Nutrition Open Science* **36**, 43–55 (2021).
- [55] Jahan-Mihan, A., Luhovyy, B. L., El Khoury, D. & Anderson, G. H. Dietary Proteins as Determinants of Metabolic and Physiologic Functions of the Gastrointestinal Tract. *Nutrients* **3**, 574–603 (2011).
- [56] van der Wielen, N. *et al.* Presence of Unabsorbed Free Amino Acids at the End of the Small Intestine of Humans and Pigs: Potential Implications for Amino Acid Bioavailability. *Current Developments in Nutrition* **5**, 530–530 (2021).
- [57] Adhikari, S., Schop, M., de Boer, I. J. M. & Huppertz, T. Protein Quality in Perspective: A Review of Protein Quality Metrics and Their Applications. *Nutrients* **14**, 947 (2022).
- [58] Knight, J., Bayram-Weston, Z. & Nigam, Y. Gastrointestinal tract 6: the effects of gut microbiota on human health. *Nursing Times* **115**, 46–50 (2019).
- [59] Huang, S., Wang, L. M., Sivendiran, T. & Bohrer, B. M. Review: Amino acid concentration of high protein food products and an overview of the current methods used to determine protein quality. *Critical Reviews in Food Science and Nutrition* **58**, 2673–2678 (2018).
- [60] Shivakumar, N. *et al.* Protein Quality Assessment of Follow-up Formula for Young Children and Ready-to-Use Therapeutic Foods: Recommendations by the FAO Expert Working Group in 2017. *The Journal of Nutrition* **150**, 195–201 (2020).
- [61] Gaudichon, C. & Calvez, J. Determinants of amino acid bioavailability from ingested protein in relation to gut health. *Current Opinion in Clinical Nutrition & Metabolic Care* **24**, 55–61 (2021).
- [62] INRAE, CIRAD & AFZ. Feed tables. <https://www.feedtables.com/>.

- [63] Moughart, S., P. J. and Gilani, Rutherford, S. M. & Tome, D. The assessment of amino acid digestibility in foods for humans and including a collation of published ileal amino acid digestibility data for human foods. Report of a Sub-Committee of the 2011 FAO Consultation on “Protein Quality Evaluation in Human Nutrition” (2011).
- [64] Kashyap, S. *et al.* Ileal digestibility of intrinsically labeled hen’s egg and meat protein determined with the dual stable isotope tracer method in indian adults. *The American Journal of Clinical Nutrition* **108**, 1319–1327 (2019).
- [65] Shivakumar, N. *et al.* Protein-quality evaluation of complementary foods in indian children. *The American Journal of Clinical Nutrition* **109**, 980–987 (2019).
- [66] Hodgkinson, S. M., Montoya, C. A., Scholten, P. T., Rutherford, S. M. & Moughan, P. J. Cooking conditions affect the true ileal digestible amino acid content and digestible indispensable amino acid score (diaas) of bovine meat as determined in pigs. *The Journal of Nutrition* **148**, 1564–1569 (2018).
- [67] Bindari, Y. R., Laerke, H. N. & Nørgaard, J. V. Standardized ileal digestibility and digestible indispensable amino acid score of porcine and bovine hydrolyzates in pigs. *Journal of the Science of Food and Agriculture* **98**, 2131–2137 (2018).
- [68] Cervantes-Pahm, S. K., Liu, Y. & Stein, H. H. Digestible indispensable amino acid score and digestible amino acids in eight cereal grains. *The British Journal of Nutrition* **111**, 1663–1672 (2014).
- [69] Reynaud, Y. *et al.* True ileal amino acid digestibility and digestible indispensable amino acid scores (DIAASs) of plant-based protein foods. *Food Chemistry* **338**, 128020 (2021).
- [70] Han, F., Moughan, P. J., Li, J. & Pang, S. Digestible indispensable amino acid scores (diaas) of six cooked chinese pulses. *Nutrients* **12**, 1183–1186 (2020).
- [71] Calvez, J. *et al.* Very low ileal nitrogen and amino acid digestibility of zein compared to whey protein isolate in healthy volunteers. *The American Journal of Clinical Nutrition* **113**, 70–82 (2021).
- [72] Tan, X. *et al.* Amino acid digestibility in housefly and black soldier fly prepupae by growing pigs. *Animal Feed Science and Technology* **263**, 114446 (2020).

- [73] Park, C. S., Helmbrecht, A., Htoo, J. K. & Adeola, O. Comparison of amino acid digestibility in full-fat soybean, two soybean meals, and peanut flour between broiler chickens and growing pigs. *Journal of Animal Science* **95**, 3110–3119 (2017).
- [74] Hugman, J. *et al.* Energy and amino acid digestibility of raw, steam-pelleted and extruded red lentil in growing pigs. *Animal Feed Science and Technology* **275**, 114838 (2021).
- [75] Bailey, H. M. & Stein, H. H. Raw and roasted pistachio nuts (*pistacia vera* l.) are ‘good’ sources of protein based on their digestible indispensable amino acid score as determined in pigs. *Journal of the Science of Food and Agriculture* **100**, 3878–3885 (2020).
- [76] Cho, K. H. *et al.* Effects of mealworm (*Tenebrio molitor*) larvae hydrolysate on nutrient ileal digestibility in growing pigs compared to those of defatted mealworm larvae meal, fermented poultry by-product, and hydrolyzed fish soluble. *Asian-Australasian Journal of Animal Sciences* **33**, 490–500 (2020).
- [77] Yin, Y. L. *et al.* Evaluating standardized ileal digestibility of amino acids in growing pigs. *Animal Feed Science and Technology* **140**, 385–401 (2008).
- [78] Kashyap, S. *et al.* True ileal digestibility of legumes determined by dual-isotope tracer method in Indian adults. *The American Journal of Clinical Nutrition* **110**, 873–882 (2019).
- [79] Wang, J. P., Kim, J. D., Kim, J. E. & Kim, I. H. Amino acid digestibility of single cell protein from *Corynebacterium ammoniagenes* in growing pigs. *Animal Feed Science and Technology* **180**, 111–114 (2013).
- [80] Zziwa, E., Laswai, G. H., Mgheni, D. M., Mtenga, L. A. & Ndikumana, J. Chemical composition and nutritional values of feed resources for ruminants. Eastern and Central Africa feed stuff table for ruminants 2013 (2013).
- [81] Oliveira, M. S. F., Wiltafsky, M. K., Lee, S. A., Kwon, W. B. & Stein, H. H. Concentrations of digestible and metabolizable energy and amino acid digestibility by growing pigs may be reduced by autoclaving soybean meal. *Animal Feed Science and Technology* **269**, 114621 (2020).
- [82] Mathai, J. K., Liu, Y. & Stein, H. H. Values for digestible indispensable amino acid scores (DIAAS) for some dairy and plant proteins may better describe protein quality than values calculated using the concept for protein digestibility-corrected amino acid scores (PDCAAS). *British Journal of Nutrition* **117**, 490–499 (2017).

- [83] Mariscal-Landin, G., Lebreton, Y. & Seve, B. Apparent and standardised true ileal digestibility of protein and amino acids from faba bean, lupin and pea, provided as whole seeds, dehulled or extruded in pig diets. *Animal Feed Science and Technology* **97**, 183–198 (2002).
- [84] Guillin, F. M. *et al.* Real ileal amino acid digestibility of pea protein compared to casein in healthy humans: a randomized trial. *The American Journal of Clinical Nutrition* **115**, 353–363 (2022).
- [85] Fanelli, N. S. *et al.* Diaas is greater in animal based burgers than in plant based burgers if determined in pigs. *European Journal of Nutrition* **61**, 461–475 (2022).
- [86] Han, F., Moughan, P. J., Li, J., Stroebinger, N. & Pang, S. The Complementarity of Amino Acids in Cooked Pulse/Cereal Blends and Effects on DIAAS. *Plants (Basel, Switzerland)* **10**, 1999 (2021).
- [87] Fanelli, N. S., Bailey, H. M., Guardiola, L. V. & Stein, H. H. Values for Digestible Indispensable Amino Acid Score (DIAAS) Determined in Pigs Are Greater for Milk Than for Breakfast Cereals, but DIAAS Values for Individual Ingredients Are Additive in Combined Meals. *The Journal of Nutrition* **151**, 540–547 (2021).
- [88] Calderón de la Barca, A. M. *et al.* Pinto Bean Amino Acid Digestibility and Score in a Mexican Dish with Corn Tortilla and Guacamole, Evaluated in Adults Using a Dual-Tracer Isotopic Method. *The Journal of Nutrition* **151**, 3151–3157 (2021).
- [89] Bailey, H. M., Mathai, J. K., Berg, E. P. & Stein, H. H. Pork Products Have Digestible Indispensable Amino Acid Scores (DIAAS) That Are Greater Than 100 When Determined in Pigs, but Processing Does Not Always Increase DIAAS. *The Journal of Nutrition* **150**, 475–482 (2020).
- [90] Devi, S. *et al.* Amino Acid Digestibility of Extruded Chickpea and Yellow Pea Protein is High and Comparable in Moderately Stunted South Indian Children with Use of a Dual Stable Isotope Tracer Method. *The Journal of Nutrition* **150**, 1178–1185 (2020).
- [91] Crosbie, M., Zhu, C., Shoveller, A. K. & Huber, L.-A. Standardized ileal digestible amino acids and net energy contents in full fat and defatted black soldier fly larvae meals (*Hermetia illucens*) fed to growing pigs. *Translational Animal Science* **4** (2020).
- [92] Rodriguez, D. A., Lee, S. A., Jones, C. K., Htoo, J. K. & Stein, H. H. Digestibility of amino acids, fiber, and energy by growing pigs, and concentrations of digestible and metabolizable energy in yellow dent corn, hard red winter wheat, and sorghum may be influenced by extrusion.

Animal Feed Science and Technology **4** (2020).

- [93] Breiman, L. Random Forests. *Machine Learning* **45**, 5–32 (2001).
- [94] Chen, T. & Guestrin, C. XGBoost: A Scalable Tree Boosting System. In *Proceedings of the 22nd ACM SIGKDD International Conference on Knowledge Discovery and Data Mining*, 785–794 (2016). ArXiv:1603.02754 [cs].
- [95] Ke, G. *et al.* LightGBM: a highly efficient gradient boosting decision tree. In *Proceedings of the 31st International Conference on Neural Information Processing Systems, NIPS'17*, 3149–3157 (Curran Associates Inc., Red Hook, NY, USA, 2017).
- [96] Azevedo, R. A., Arruda, P., Turner, W. L. & Lea, P. J. The biosynthesis and metabolism of the aspartate derived amino acids in higher plants. *Phytochemistry* **46**, 395–419 (1997).
- [97] Kohlmeier, M. *Nutrient Metabolism* (Academic Press, London, 2003).
- [98] He, J. *et al.* The effect of meat processing methods on changes in disulfide bonding and alteration of protein structures: impact on protein digestion products. *RSC Advances* **8**, 17595–17605 (2018).
- [99] Knorr, D. Effect of recovery methods on yield, quality and functional properties of potato protein concentrates. *Journal of Food Science* **45**, 1183–1186 (1980).
- [100] Saltelli, A. *et al.* Variance based sensitivity analysis of model output. design and estimator for the total sensitivity index. *Computer Physics Communications* **181**, 259–270 (2010).
- [101] Usher, W. *et al.* Salib/Salib: Launch! (2016). <https://zenodo.org/record/160164>.
- [102] House, J. D., Hill, K., Neufeld, J., Franczyk, A. & Nosworthy, M. G. Determination of the protein quality of almonds (*Prunus dulcis* L.) as assessed by in vitro and in vivo methodologies. *Food Science & Nutrition* **7**, 2932–2938 (2019).
- [103] AFZ, Ajinomoto Eurolysine, Aventis Animal Nutrition, INRA & ITCF. *Amipig: ileal standardised digestibility of amino acids in feedstuffs for pigs* (France, 2000).
- [104] GenomeNet. Aaindex ver.9.2 URL https://www.genome.jp/aaindex/AAindex/list_of_indices.

5 Supplementary Material

5.1 Protein quality and bioavailability definition

To define the pattern of human AA requirements, the FAO Committee on Protein Requirements [52] advised using a reference protein with an ideal AA composition.

The balance of AA across the small intestine (mouth to terminal ileum: ileal digestibility) or across the entire gut (mouth to anus: faecal digestibility) can provide a measure of the extent of digestion and absorption of food protein. Specifically, this balance is usually defined in terms of AA by the gastrointestinal tract for use by the body. Usually, the main interest of the analyses are the indispensable amino acids (IAAs), which cannot be synthesized by the human body and some dispensable amino acids (DAAs), such as arginine, cysteine, glutamine, glycine, proline and tyrosine, which can become conditionally indispensable for premature neonates [53].

Protein digestion is a long, complex and multi-stage process. The onset is from the mechanical process of breaking down food in the mouth and the chemical process of breaking down the molecular structure by salivary amylase. In the gastric phase of digestion, the resulting product is mixed with low pH gastric acid containing the protease pepsin. This allows the formation of (poly)peptides. In the small intestine, the chyme is mixed with pancreatic proteases and peptidases, such as trypsin, chymotrypsin, and carboxypeptidase A [54]. Together with intestinal brush border enzymes, these enzymes hydrolyse the proteins and (poly)peptides into amino acids, di-, tri-, and oligopeptides [55]. The amino acids and di- and tripeptides that are produced can be taken up by the small intestinal mucosa and are typically thought to be almost completely absorbed by the terminal ileum at the end of the small intestine [56, 57]. It is important to mention that this is a unique process that depends on the individual gut microbiota, which plays an active role in digestion [58].

Peptides not absorbed in the ileum travel to the large intestine. However, there is no evidence that there is absorption of them after the ileum, and the absorbed values are small, not exceeding 0.1% for whey protein in pigs [56]. Many different methods for determining protein quality have been developed and utilized throughout the years. To quantify or characterize the protein quality of a protein supply, several approaches use distinct principles [59].

FAO [60] suggested a ranking of different digesta based on representativeness to human digestibility for protein starts with human ileal digesta, followed by pig ileal digesta, rat ileal digesta, human faecal digesta, pig faecal digesta and rat faecal digesta. Some human experiments have been conducted to test the ileal digestibility of proteins, however the ileal digesta collection in animals is difficult [61]. Generally, pigs are used over humans because of the physiological similarity of their intestinal tract. Furthermore, there is a high correlation between ileal digesta from humans and pigs [36].

5.2 References of DIAAS experiments

	Paper	Reference
	INRAE-CIRAD-AFZ Feed tables	62
	The assessment of amino acid digestibility in foods for humans and including a collation of published ileal amino acid digestibility data for human foods	63
	Ileal digestibility of intrinsically labelled hen's egg and meat protein determined with the dual stable isotope tracer method in Indian adults	64
	Protein quality evaluation of complementary foods in Indian children	65
	Cooking conditions affect the true ileal digestible amino acid content and digestible indispensable amino acid score (DIAAS) of bovine meat as determined in pigs	66
	Standardized ileal digestibility and digestible indispensable amino acid score of porcine and bovine hydrolysates in pigs	67
	Digestible indispensable amino acid score and digestible indispensable amino acid score of porcine and bovine hydrolysates in pigs	68
	True ileal amino acid digestibility and digestible indispensable amino acid scores (DIAASs) of plant-based protein foods	69
	Digestible indispensable amino acid scores of six cooked chinese pulses	70
	Very low ileal nitrogen and amino acid digestibility of zein compared to whey protein isolate in healthy volunteers	71
	Amino acid digestibility in housefly and black soldier fly prepupae by growing pigs	72
	Comparison of amino acid digestibility in full-fat soybean, two soybean meals and peanut flour between broiler chickens and growing pigs	73
	Energy and amino acid digestibility of raw, steam-pelleted and extruded red lentil in growing pigs	74
	Raw and roasted pistachio nuts are good sources of protein based on their digestible indispensable amino acid score as determined in pigs	75
	Effects of mealworm larvae hydrolysate on nutrient ileal digestibility in growing pigs compared to those of defatted mealworm larvae meal, fermented poultry byproduct and hydrolysed fish soluble	76
	Evaluating standardized ileal digestibility of amino acids in growing pigs	77
	True ileal digestibility of legumes determined by dual-isotope tracer method in Indian adults	78
	Amino acid digestibility of single cell protein from <i>Corynebacterium</i>	79
	Chemical composition and nutritional values of feedstuffs	80
	Concentrations of digestible and metabolizable energy and amino acid digestibility by growing pigs may be reduced by autoclaving soybean meal	81
	Values for DIAAS for some dairy and plant proteins may better describe protein quality than values calculated using the concept for PDCAAS	82
	Apparent and standardized true ileal digestibility of protein and amino acids from faba bean, lupin and pea, provided as whole seeds, dehulled or extruded in pig diets	83
	Real ileal amino acid digestibility of pea protein compared to casein in healthy humans, a randomized trial	84
	DIAAS is greater in animal based burgers than in plant based burgers if determined in pigs	85
	The complementarity of amino acids in cooked pulse/cereal blends and effects on DIAAS	86
	Values for DIAAS determined in pigs are greater for milk than for breakfast cereals, but DIAAS values for individual ingredients are additive in combined meals	87
	Pinto bean amino acid digestibility and score in a Mexican dish with corn tortilla and guacamole, evaluated in adults using a dual tracer isotopic method	88
	Most meat products have DIAAS that are greater than 100, but processing may increase or reduce protein quality	89
	Amino Acid Digestibility of Extruded Chickpea and Yellow Pea Protein is High and Comparable in Moderately Stunted South Indian Children with Use of a Dual Stable Isotope Tracer Method	90
	Standardized ileal digestible amino acids and net energy contents in full fat and defatted black soldier fly larvae meals (<i>Hermetia illucens</i>) fed to growing pigs	91
	Digestibility of amino acids, fiber, and energy by growing pigs, and concentrations of digestible and metabolizable energy in yellow dent corn, hard red winter wheat, and sorghum may be influenced by extrusion	92

Table 2 References used to obtain the DIAAS values of almost 200 food items.

5.3 Features added to the dataset

Feature	Unit
Protein	g/kg
Tryptophan (TRP)	g/kg
Threonine (THR)	g/kg
Isoleucine (ILE)	g/kg
Leucine (LEU)	g/kg
Lysine (LYS)	g/kg
Methionine (MET)	g/kg
Cysteine (CYS)	g/kg
Phenylalanine (PHE)	g/kg
Tyrosine (TYR)	g/kg
Valine (VAL)	g/kg
Arginine (ARG)	g/kg
Histidine (HIS)	g/kg

Table 3 Total protein content and AAS are the features obtained for each food item in the training dataset.

Feature	Unit
Energy	kJ/100g
Dietary Fiber	g/100g
Fat	g/100g
Ash	g/100g
Total Sugar	g/100g
Calcium	mg/100g
Sodium	mg/100g
Manganese	mg/100g
Zinc	mg/100g
Copper	mg/100g
Iron	mg/100g
Selenium	ug/100g

Table 4 Nutritional information added to each food item in the training dataset.

5.4 Baseline models accuracy

Random forest is an ensemble of decision trees created by using bootstrap samples of the training dataset and random selection in tree induction [93]. XGBoost is an ensemble approach with a gradient descent–boosted decision tree algorithm [94]. LightGBM is an improvement framework based on the gradient descent–boosted decision tree algorithm and is more powerful than the previous XGBoost with a fast training speed and less memory occupation [95].

Model	R^2	RSME
LGBM	0.88	0.04
XGBoost	0.87	0.04
Random Forest	0.82	0.05
Gradient Boosting	0.82	0.05
Bagging	0.81	0.05
KNeighbors	0.73	0.06
Decision Tree	0.72	0.06
Nu Support Vector Regression	0.70	0.07
Linear Regression	0.66	0.07
Lasso model (with Lars)	0.66	0.07
SVR	0.62	0.07
Poisson	0.49	0.09

Table 5 Root mean squared error (RMSE) and R^2 for each baseline model. All the hyperparameters were set to the default parameters of Scikit-learn. No feature selection was applied i.e., all features were used.

5.5 Interpretability of feature impact for food item

Using SHAP interaction values, we can decompose the impact of a feature on a specific sample, allowing for model interpretability. We selected three of the food items we predicted the true ileal digestibility and plot the contributions of each feature in the model for this specific sample, as shown in Supplementary figure 4.

It is known that maize protein quality is fairly poor because it contains very low amounts of the essential amino threonine (THR) [96]. Tyrosine values were also not reported in our dataset, mainly because it's usually present in high amount on maize [97]. These and the dietary fiber content are negatively impacting the model. The hydrophobicity of the proteins of maize on the other hand, increase protein digestibility. It is known that an increase in protein hydrophobicity is directly related to protein unfolding and positively correlated with digestion [22, 98]. The same characteristic is observed on Pork. Thus, the small values of dietary fiber and magnesium of the food item also increased the protein digestibility.

For potato protein concentrate, the amount of total protein is directly associated with the protein digestibility. The low values of dietary fiber also impacted the model positively and potatoes are usually high on lysine [99]. Tofu's low levels of magnesium, potassium and dietary fiber increased the protein digestibility prediction. The original soy milk is heated during tofu's production process, which might lead to protein unfolding and an increase in protein hydrophobicity as well.

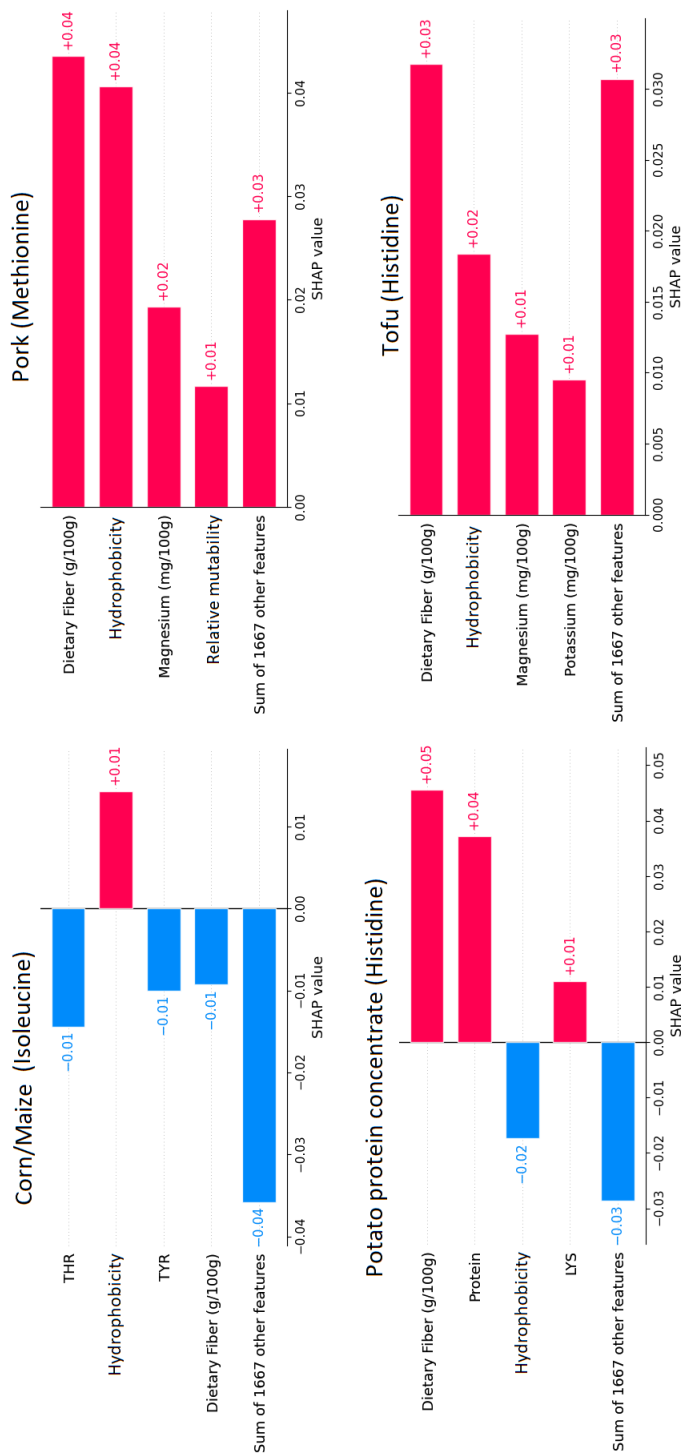


Fig. 4

Limiting amino acid predicted for food items

Food Item	Limiting amino acid	
	DIAAS for Infants	DIAAS for Children
Corn/Maize	Tryptophan	Lysine
Soybean protein concentrate	Leucine	Lysine
Potato protein concentrate	Tryptophan	Histidine
Tofu	SAAs	SAAs
Rye (Secale cereale L.)	Tryptophan	Lysine
Pork (raw belly)	Tryptophan	Valine
Almond	Cysteine	Cysteine

Table 6 Limiting amino acid of each food item for each DIAAS category, considering the reference vales. SAAs represent the sulphur-containing amino acids.

5.6 Ablation study

Figure 5 shows the inputs that the different models were created with. For each model, we used 2304 samples, determined by the true ileal digestibility of the 12 indispensable aminoacids of 192 food items. Model A, also known as the baseline model, was trained using the complete dataset composed of 10700 features, such as nutritional information, amino acid score, and biochemical information obtained through protein sequence. Model B was trained with 25 features after the selection of the 20 most important features using SHAP. For model C we used these same 20 features with the 3 families of 1024 embeddings obtained from the language model, resulting in 3097 features. Hyperparameters of all these models were optimized using a combination of a randomized grid search technique and manual tuning using stratified 5-fold cross-validation on the training set.

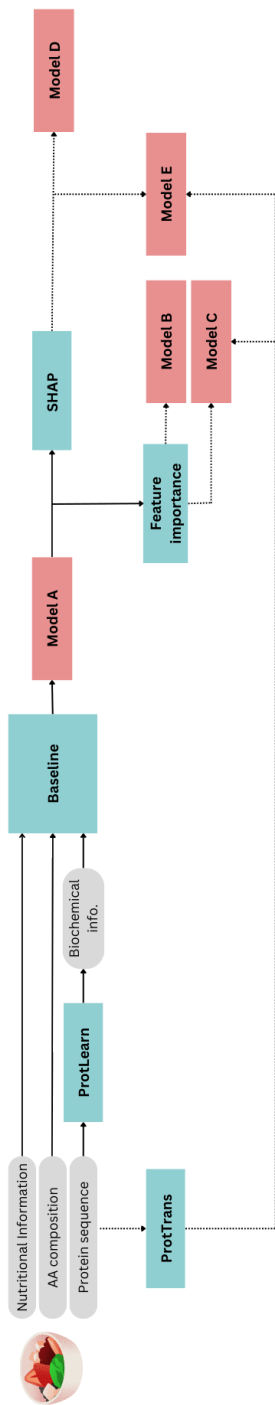


Fig. 5 Architecture of the ablation study. The baseline model (A) is trained using nutritional information, AA composition and the biochemical features extracted from the protein sequences, using Protlearn. The most important features are selected using the feature importance from LGBM (model B) and the embeddings of the transformer model are added to the dataset (model C). Then, the feature importance is substituted by the Shapley (SHAP) method, when model D is trained without the embeddings and model E is trained with the embeddings.

5.7 Sensitivity Analysis

In this section, we report the results of sensitivity analysis to study how the uncertainty in the model output is explained by the different input features. We use a variance based sensitivity analysis method as described in [100]. We used the SALib package [101] for sensitivity analysis. Figure 6 illustrates the results of sensitivity analysis. We report the total order sensitivity effects that measure the variance in the output due to the first-order effects (by varying the input alone) and its interactions with other features. We observe that ProtTrans embeddings obtained by training on the protein sequences explained the maximum amount of variation (52%) in the digestibility coefficient, our output. The remaining variation was contributed to by the nutritional (36%), biochemical (0.04%) and categorical features that include the protein families, food group and indispensable amino acid related inputs (29%).

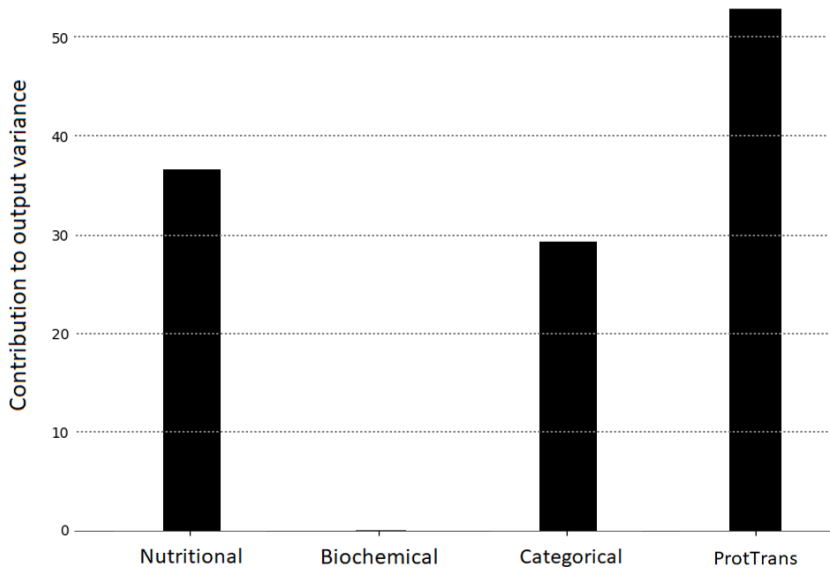


Fig. 6 Results of sensitivity analysis. On the x axis are the inputs that we grouped as follows: nutritional, biochemical, categorical (including the protein families, food group and indispensable amino acid related features), and, ProTrans embeddings. The y axis shows the contribution of each of these input groups to the variance in the output i.e. the digestibility coefficient.

DIAAS value calculation

To calculate the DIAAS value obtained through the predicted true ileal digestibility coefficient of each amino acid, the following equation is used:

$$\text{DIAAS}[\%] = 100 \frac{\text{IAA}_T}{\text{IAA}_R} \quad (1)$$

where IAA_T is mg of digestible dietary IAA in 1 gram of the test protein and IAA_R is the amount of mg of the same amino acid in 1 gram of the reference IAA. The digestible dietary content of each IAA is calculated as the content of each amino acid multiplied by their respective digestibility coefficient or true ileal digestibility score. The amount of each IAA in the reference protein is calculated by dividing the requirement for each IAA by the estimated average requirement. Thus, the DIAAS is determined by the most limiting IAA in the test protein in relation to its corresponding content in the reference protein.

Supplementary table 7 shows the DIAAS for infants, children and adults calculated for 7 different food items. The ground truth values were obtained through experiments and referenced on the table. These values were calculated out of the predicted true ileal digestibility values for each amino acid. The limiting amino acids of each food item for each DIAAS category is shown in Supplementary table 6. An example of the calculated values for almond is shown in figure 7.

To our knowledge, DIAAS has not been determined in almonds. However, PDCAAS values ranged from 44.3 to 47.8 [102]. However, PDCAAS values were reported to be generally higher than a DIAAS values, especially for the poorer quality proteins. Therefore, having DIAAS values for as many food items as possible are of potential practical importance for populations in which dietary protein intake may be marginal [9].

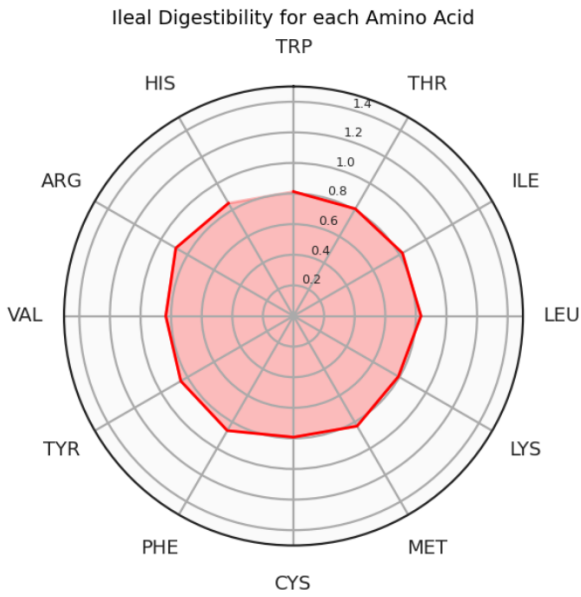


Fig. 7 Radar plot of the true ileal digestibility for each amino acid for almond. The obtained values are 0.81 for tryptophan and threonine, 0.82 for isoleucine, 0.83 for leucine and methionine, 0.79 for lysine and cysteine, 0.87 for phenylalanine, 0.85 for valine and histidine and 0.89 for arginine.

DIAAS value of food items

Food Item	Origin	Reference	DIAAS for Infants		DIAAS for Children		DIAAS for Adults	
			Ground Truth	Predicted	Ground Truth	Predicted	Ground Truth	Predicted
Maize (yellow dent)	Train	[68]	27	29.91	40	39.65	48	47.09
Soybean protein concentrate	Train	[103]	76	75.32	102	102.20	112	112.10
Potato protein concentrate	Test	[103]	61	68.26	95	93.73	118	117.17
Tofu	Test	[69]	62	65.92	75	80.57	88	94.58
Rye (Secale cereale L.)	Test	[68]	41	40.69	50	51.85	60	61.57
Pork (raw belly)	Test	[89]	69	66.76	110	109.92	119	118.16
Almond	-	-	No data available	31.00	No data available	37.00	No data available	44.00

Table 7 A few examples of DIAAS values predicted with our approach. Seven food items were selected from train, test and outside both train and test datasets. The ground truth for each was obtained from the references through experiments and the values of DIAAS for Infants, Children and Adults were calculated.

5.8 Biological and physiochemical features extracted from Protlearn

The following table summarizes the features we extracted from the Protlearn package [15]. For each food item in our dataset, we collected 2 to 3 FASTA sequences of their most abundant protein families. By inputting each FASTA sequence into the Protlearn [15] package, we obtained several features of that chemically and physically characterized the component protein families of each food. The large majority of these extracted features are Amino Acid Indices, a set of 566 indices [15] [104] that represent various physiochemical properties of amino acids. The indices for each protein sequence are calculated by averaging the index values for all of the individual amino acids in the sequence.

Feature	Descriptor
Entropy	The Shannon entropy for the amino acid sequence
C	Fraction of carbon atoms
H	Fraction of hydrogen atoms
N	Fraction of nitrogen atoms
O	Fraction of oxygen atoms
S	Fraction of sulfur atoms
N	Fraction of nitrogen atoms
Total Bound	Total number of bonds
Single Bound	Number of single bonds
Double Bound	Number of double bonds
ANDN920101	alpha-CH chemical shifts
ARGP820101	Hydrophobicity index
ARGP820102	Signal sequence helical potential
ARGP820103	Membrane-buried preference parameters
BEGF750101	Conformational parameter of inner helix
BEGF750102	Conformational parameter of beta-structure
BEGF750103	Conformational parameter of beta-turn
BHAR880101	Average flexibility indices
BIGC670101	Residue volume
BIOV880101	Information value for accessibility; average fraction 35%
BIOV880102	Information value for accessibility; average fraction 23%
BROC820101	Retention coefficient in TFA
BROC820102	Retention coefficient in HFBA
BULH740101	Transfer free energy to surface
BULH740102	Apparent partial specific volume
BUNA790101	alpha-NH chemical shifts
BUNA790102	alpha-CH chemical shifts
BUNA790103	Spin-spin coupling constants 3JH _{alpha} -NH
BURA740101	Normalized frequency of alpha-helix
BURA740102	Normalized frequency of extended structure
CHAM810101	Steric parameter
CHAM820101	Polarizability parameter
CHAM820102	Free energy of solution in water, kcal/mole
CHAM830101	The Chou-Fasman parameter of the coil conformation
CHAM830102	A parameter defined from the residuals obtained from the best correlation of the Chou-Fasman parameter of beta-sheet

Feature	Descriptor
CHAM830103	The number of atoms in the side chain labelled 1 + 1
CHAM830104	The number of atoms in the side chain labelled 2 + 1
CHAM830105	The number of atoms in the side chain labelled 3 + 1
CHAM830106	The number of bonds in the longest chain
CHAM830107	A parameter of charge transfer capability
CHAM830108	A parameter of charge transfer donor capability
CHOC750101	Average volume of buried residue
CHOC760101	Residue accessible surface area in tripeptide
CHOC760102	Residue accessible surface area in folded protein
CHOC760103	Proportion of residues 95% buried
CHOC760104	Proportion of residues 100% buried
CHOP780101	Normalized frequency of beta-turn
CHOP780201	Normalized frequency of alpha-helix
CHOP780202	Normalized frequency of beta-sheet
CHOP780203	Normalized frequency of beta-turn
CHOP780204	Normalized frequency of N-terminal helix
CHOP780205	Normalized frequency of C-terminal helix
CHOP780206	Normalized frequency of N-terminal non helical region
CHOP780207	Normalized frequency of C-terminal non helical region
CHOP780208	Normalized frequency of N-terminal beta-sheet
CHOP780209	Normalized frequency of C-terminal beta-sheet
CHOP780210	Normalized frequency of N-terminal non beta region
CHOP780211	Normalized frequency of C-terminal non beta region
CHOP780212	Frequency of the 1st residue in turn
CHOP780213	Frequency of the 2nd residue in turn
CHOP780214	Frequency of the 3rd residue in turn
CHOP780215	Frequency of the 4th residue in turn
CHOP780216	Normalized frequency of the 2nd and 3rd residues in turn
CIDH920101	Normalized hydrophobicity scales for alpha-proteins
CIDH920102	Normalized hydrophobicity scales for beta-proteins
CIDH920103	Normalized hydrophobicity scales for alpha+beta-proteins
CIDH920104	Normalized hydrophobicity scales for alpha/beta-proteins
CIDH920105	Normalized average hydrophobicity scales
COHE430101	Partial specific volume

Feature	Descriptor
CIDH920104	Normalized hydrophobicity scales for alpha/beta-proteins
CIDH920105	Normalized average hydrophobicity scales
COHE430101	Partial specific volume
CRAJ730101	Normalized frequency of middle helix
CRAJ730102	Normalized frequency of beta-sheet
CRAJ730103	Normalized frequency of turn
DAWD720101	Size
DAYM780101	Amino acid composition
DAYM780201	Relative mutability
DESM900101	Membrane preference for cytochrome b: MPH89
DESM900102	Average membrane preference: AMP07
EISD840101	Consensus normalized hydrophobicity scale
EISD860101	Solvation free energy
EISD860102	Atom-based hydrophobic moment
EISD860103	Direction of hydrophobic moment
FASG760101	Molecular weight
FASG760102	Melting point
FASG760103	Optical rotation
FASG760104	pK-N
FASG760105	pK-C
FAUJ830101	Hydrophobic parameter pi
FAUJ880101	Graph shape index
FAUJ880102	Smoothed epsilon steric parameter
FAUJ880103	Normalized van der Waals volume
FAUJ880104	STERIMOL length of the side chain
FAUJ880105	STERIMOL minimum width of the side chain
FAUJ880106	STERIMOL maximum width of the side chain
FAUJ880107	N.m.r. chemical shift of alpha-carbon
FAUJ880108	Localized electrical effect
FAUJ880109	Number of hydrogen bond donors
FAUJ880110	Number of full nonbonding orbitals
FAUJ880111	Positive charge
FAUJ880112	Negative charge
FAUJ880113	pK-a(RCOOH)
FINA770101	Helix-coil equilibrium constant
FINA910101	Helix initiation parameter at position $i - 1$
FINA910102	Helix initiation parameter at position $i, i + 1, i + 2$
FINA910103	Helix termination parameter at position $j - 2, j - 1, j$
FINA910104	Helix termination parameter at position $j + 1$
GARJ730101	Partition coefficient
GEIM800101	Alpha-helix indices

Feature	Descriptor
GEIM800102	Alpha-helix indices for alpha-proteins
GEIM800103	Alpha-helix indices for beta-proteins
GARJ730101	Partition coefficient
GEIM800101	Alpha-helix indices
GEIM800102	Alpha-helix indices for alpha-proteins
GEIM800103	Alpha-helix indices for beta-proteins
GEIM800104	Alpha-helix indices for alpha/beta-proteins
GEIM800105	Beta-strand indices
GEIM800106	Beta-strand indices for beta-proteins
GEIM800107	Beta-strand indices for alpha/beta-proteins
GEIM800108	Aperiodic indices
GEIM800109	Aperiodic indices for alpha-proteins
GEIM800110	Aperiodic indices for beta-proteins
GEIM800111	Aperiodic indices for alpha/beta-proteins
GOLD730101	Hydrophobicity factor
GOLD730102	Residue volume
GRAR740101	Composition
GRAR740102	Polarity
GRAR740103	Volume
GUYH850101	Partition energy
HOPA770101	Hydration number
HOPT810101	Hydrophilicity value
HUTJ700101	Heat capacity
HUTJ700102	Absolute entropy
HUTJ700103	Entropy of formation
ISOY800101	Normalized relative frequency of alpha-helix
ISOY800102	Normalized relative frequency of extended structure
ISOY800103	Normalized relative frequency of bend
ISOY800104	Normalized relative frequency of bend R
ISOY800105	Normalized relative frequency of bend S
ISOY800106	Normalized relative frequency of helix end
ISOY800107	Normalized relative frequency of double bend
ISOY800108	Normalized relative frequency of coil
JANJ780101	Average accessible surface area
JANJ780102	Percentage of buried residues
JANJ780103	Percentage of exposed residues
JANJ790101	Ratio of buried and accessible molar fractions
JANJ790102	Transfer free energy
JOND750101	Hydrophobicity
JOND750102	pK (-COOH)
JOND920101	Relative frequency of occurrence
JOND920102	Relative mutability

Feature	Descriptor
JUKT750101	Amino acid distribution
JUNJ780101	Sequence frequency
KANM800101	Average relative probability of helix
KANM800102	Average relative probability of beta-sheet
KANM800103	Average relative probability of inner helix
KANM800104	Average relative probability of inner beta-sheet
KARP850101	Flexibility parameter for no rigid neighbors
KARP850102	Flexibility parameter for one rigid neighbor
KARP850103	Flexibility parameter for two rigid neighbors
KHAG800101	The Kerr-constant increments
KLEP840101	Net charge
KRIW710101	Side chain interaction parameter
KRIW790101	Side chain interaction parameter
KRIW790102	Fraction of site occupied by water
KRIW790103	Side chain volume
KY TJ820101	Hydropathy index
LAW E840101	Transfer free energy, CHP/water
LEVM760101	Hydrophobic parameter
LEVM760102	Distance between C-alpha and centroid of side chain
LEVM760103	Side chain angle theta(AAR)
LEVM760104	Side chain torsion angle phi(AAAR)
LEVM760105	Radius of gyration of side chain
LEVM760106	van der Waals parameter R0
LEVM760107	van der Waals parameter epsilon
LEVM780101	Normalized frequency of alpha-helix, with weights
LEVM780102	Normalized frequency of beta-sheet, with weights
LEVM780103	Normalized frequency of reverse turn, with weights
LEVM780104	Normalized frequency of alpha-helix, unweighted
LEVM780106	Normalized frequency of reverse turn, unweighted
LEWP710101	Frequency of occurrence in beta-bends
LIFS790101	Conformational preference for all beta-strands
LIFS790102	Conformational preference for parallel beta-strands
LIFS790103	Conformational preference for antiparallel beta-strands
MANP780101	Average surrounding hydrophobicity
MAXF760101	Normalized frequency of alpha-helix
MAXF760102	Normalized frequency of extended structure
MAXF760103	Normalized frequency of zeta R
MAXF760104	Normalized frequency of left-handed alpha-helix
MAXF760105	Normalized frequency of zeta L
MAXF760106	Normalized frequency of alpha region
MCMT640101	Refractivity
MEEJ800101	Retention coefficient in HPLC, pH7.4
MEEJ800102	Retention coefficient in HPLC, pH2.1

Feature	Descriptor
MEEJ810101	Retention coefficient in NaClO ₄
MEEJ810102	Retention coefficient in NaH ₂ PO ₄
MEIH800101	Average reduced distance for C-alpha
MEIH800102	Average reduced distance for side chain
MEIH800103	Average side chain orientation angle
MIYS850101	Effective partition energy
NAGK730101	Normalized frequency of alpha-helix
NAGK730102	Normalized frequency of beta-structure
NAGK730103	Normalized frequency of coil
NAKH900101	AA composition of total proteins
NAKH900102	SD of AA composition of total proteins
NAKH900103	AA composition of mt-proteins
NAKH900104	Normalized composition of mt-proteins
NAKH900105	AA composition of mt-proteins from animal
NAKH900106	Normalized composition from animal
NAKH900107	AA composition of mt-proteins from fungi and plant
NAKH900108	Normalized composition from fungi and plant
NAKH900109	AA composition of membrane proteins
NAKH900110	Normalized composition of membrane proteins
NAKH900111	Transmembrane regions of non-mt-proteins
NAKH900112	Transmembrane regions of mt-proteins
NAKH900113	Ratio of average and computed composition
NAKH920101	AA composition of CYT of single-spanning proteins
NAKH920102	AA composition of CYT2 of single-spanning proteins
NAKH920103	AA composition of EXT of single-spanning proteins
NAKH920104	AA composition of EXT2 of single-spanning proteins
NAKH920105	AA composition of MEM of single-spanning proteins
NAKH920106	AA composition of CYT of multi-spanning proteins
NAKH920107	AA composition of EXT of multi-spanning proteins
NAKH920108	AA composition of MEM of multi-spanning proteins
NISK800101	8 Å contact number
NISK860101	14 Å contact number
NOZY710101	Transfer energy, organic solvent/water
OOBM770101	Average non-bonded energy per atom
OOBM770102	Short and medium range non-bonded energy per atom
OOBM770103	Long range non-bonded energy per atom
OOBM770104	Average non-bonded energy per residue
OOBM770105	Short and medium range non-bonded energy per residue
OOBM850101	Optimized beta-structure-coil equilibrium constant
OOBM850102	Optimized propensity to form reverse turn
OOBM850103	Optimized transfer energy parameter

Feature	Descriptor
OOBM850104	Optimized average non-bonded energy per atom
OOBM850105	Optimized side chain interaction parameter
PALJ810101	Normalized frequency of alpha-helix from LG
PALJ810102	Normalized frequency of alpha-helix from CF
PALJ810103	Normalized frequency of beta-sheet from LG
PALJ810104	Normalized frequency of beta-sheet from CF
PALJ810105	Normalized frequency of turn from LG
PALJ810106	Normalized frequency of turn from CF
PALJ810107	Normalized frequency of alpha-helix in all-alpha class
PALJ810108	Normalized frequency of alpha-helix in alpha+beta class
PALJ810109	Normalized frequency of alpha-helix in alpha/beta class
PALJ810110	Normalized frequency of beta-sheet in all-beta class
PALJ810111	Normalized frequency of beta-sheet in alpha+beta class
PALJ810112	Normalized frequency of beta-sheet in alpha/beta class
PALJ810113	Normalized frequency of turn in all-alpha class
PALJ810114	Normalized frequency of turn in all-beta class
PALJ810115	Normalized frequency of turn in alpha+beta class
PALJ810116	Normalized frequency of turn in alpha/beta class
PARJ860101	HPLC parameter
PLIV810101	Partition coefficient
PONP800101	Surrounding hydrophobicity in folded form
PONP800102	Average gain in surrounding hydrophobicity
PONP800103	Average gain ratio in surrounding hydrophobicity
PONP800104	Surrounding hydrophobicity in alpha-helix
PONP800105	Surrounding hydrophobicity in beta-sheet
PONP800106	Surrounding hydrophobicity in turn
PONP800107	Accessibility reduction ratio
PONP800108	Average number of surrounding residues
PRAM820101	Intercept in regression analysis
PRAM820102	Slope in regression analysis x 1.0E1
PRAM820103	Correlation coefficient in regression analysis
PRAM900101	Hydrophobicity
PRAM900102	Relative frequency in alpha-helix
PRAM900103	Relative frequency in beta-sheet
PRAM900104	Relative frequency in reverse-turn
PTIO830101	Helix-coil equilibrium constant

Feature	Descriptor
PONP800103	Average gain ratio in surrounding hydrophobicity
PONP800104	Surrounding hydrophobicity in alpha-helix
PONP800105	Surrounding hydrophobicity in beta-sheet
PONP800106	Surrounding hydrophobicity in turn
PONP800107	Accessibility reduction ratio
PONP800108	Average number of surrounding residues
PRAM820101	Intercept in regression analysis
PRAM820102	Slope in regression analysis $\times 1.0E1$
PTIO830102	Beta-coil equilibrium constant
QIAN880101	Weights for alpha-helix at the window position of -6
QIAN880102	Weights for alpha-helix at the window position of -5
QIAN880103	Weights for alpha-helix at the window position of -4
QIAN880104	Weights for alpha-helix at the window position of -3
QIAN880105	Weights for alpha-helix at the window position of -2
QIAN880106	Weights for alpha-helix at the window position of -1
QIAN880107	Weights for alpha-helix at the window position of 0
QIAN880108	Weights for alpha-helix at the window position of 1
QIAN880109	Weights for alpha-helix at the window position of 2
QIAN880110	Weights for alpha-helix at the window position of 3
QIAN880111	Weights for alpha-helix at the window position of 4
QIAN880112	Weights for alpha-helix at the window position of 5
QIAN880113	Weights for alpha-helix at the window position of 6
QIAN880114	Weights for beta-sheet at the window position of -6
QIAN880115	Weights for beta-sheet at the window position of -5
QIAN880116	Weights for beta-sheet at the window position of -4
QIAN880117	Weights for beta-sheet at the window position of -3
QIAN880118	Weights for beta-sheet at the window position of -2
QIAN880119	Weights for beta-sheet at the window position of -1
QIAN880120	Weights for beta-sheet at the window position of 0
QIAN880121	Weights for beta-sheet at the window position of 1
QIAN880122	Weights for beta-sheet at the window position of 2
QIAN880123	Weights for beta-sheet at the window position of 3
QIAN880124	Weights for beta-sheet at the window position of 4
QIAN880125	Weights for beta-sheet at the window position of 5
QIAN880126	Weights for beta-sheet at the window position of 6
QIAN880127	Weights for coil at the window position of -6
QIAN880128	Weights for coil at the window position of -5
QIAN880129	Weights for coil at the window position of -4
QIAN880130	Weights for coil at the window position of -3
QIAN880131	Weights for coil at the window position of -2
QIAN880132	Weights for coil at the window position of -1
QIAN880133	Weights for coil at the window position of 0

Feature	Descriptor
QIAN880134	Weights for coil at the window position of 1
QIAN880135	Weights for coil at the window position of 2
QIAN880136	Weights for coil at the window position of 3
QIAN880137	Weights for coil at the window position of 4
QIAN880138	Weights for coil at the window position of 5
QIAN880139	Weights for coil at the window position of 6
RACS770101	Average reduced distance for C-alpha
RACS770102	Average reduced distance for side chain
RACS770103	Side chain orientational preference
RACS820101	Average relative fractional occurrence in A0(i)
RACS820102	Average relative fractional occurrence in AR(i)
RACS820103	Average relative fractional occurrence in AL(i)
RACS820104	Average relative fractional occurrence in EL(i)
RACS820105	Average relative fractional occurrence in E0(i)
RACS820106	Average relative fractional occurrence in ER(i)
RACS820107	Average relative fractional occurrence in A0(i-1)
RACS820108	Average relative fractional occurrence in AR(i-1)
RACS820109	Average relative fractional occurrence in AL(i-1)
RACS820110	Average relative fractional occurrence in EL(i-1)
RACS820111	Average relative fractional occurrence in E0(i-1)
RACS820112	Average relative fractional occurrence in ER(i-1)
RACS820113	Value of theta(i)
RACS820114	Value of theta(i-1)
RADA880101	Transfer free energy from chx to wat
RADA880102	Transfer free energy from oct to wat
RADA880103	Transfer free energy from vap to chx
RADA880104	Transfer free energy from chx to oct
RADA880105	Transfer free energy from vap to oct
RADA880106	Accessible surface area
RADA880107	Energy transfer from out to in(95%buried)
RADA880108	Mean polarity
RICJ880101	Relative preference value at N''
RICJ880102	Relative preference value at N'
RICJ880103	Relative preference value at N-cap
RICJ880104	Relative preference value at N1
RICJ880105	Relative preference value at N2
RICJ880106	Relative preference value at N3
RICJ880107	Relative preference value at N4
RICJ880108	Relative preference value at N5
RICJ880109	Relative preference value at Mid
RICJ880110	Relative preference value at C5
RICJ880111	Relative preference value at C4
RICJ880112	Relative preference value at C3

Feature	Descriptor
RICJ880113	Relative preference value at C2
RICJ880114	Relative preference value at C1
RICJ880115	Relative preference value at C-cap
RICJ880116	Relative preference value at C'
RICJ880117	Relative preference value at C''
ROBB760101	Information measure for alpha-helix
ROBB760102	Information measure for N-terminal helix
ROBB760103	Information measure for middle helix
ROBB760104	Information measure for C-terminal helix
ROBB760105	Information measure for extended
ROBB760106	Information measure for pleated-sheet
ROBB760107	Information measure for extended without H-bond
ROBB760108	Information measure for turn
ROBB760109	Information measure for N-terminal turn
ROBB760110	Information measure for middle turn
ROBB760111	Information measure for C-terminal turn
ROBB760112	Information measure for coil
ROBB760113	Information measure for loop
ROBB790101	Hydration free energy
ROSG850101	Mean area buried on transfer
ROSG850102	Mean fractional area loss
ROSM880101	Side chain hydropathy, uncorrected for solvation
ROSM880102	Side chain hydropathy, corrected for solvation
ROSM880103	Loss of Side chain hydropathy by helix formation
SIMZ760101	Transfer free energy
SNEP660101	Principal component I
SNEP660102	Principal component II
SNEP660103	Principal component III
SNEP660104	Principal component IV
SUEM840101	Zimm-Bragg parameter s at 20 C
SUEM840102	Zimm-Bragg parameter sigma x 1.0E4
SWER830101	Optimal matching hydrophobicity
TANS770101	Normalized frequency of alpha-helix
TANS770102	Normalized frequency of isolated helix
TANS770103	Normalized frequency of extended structure
TANS770104	Normalized frequency of chain reversal R
TANS770105	Normalized frequency of chain reversal S
TANS770106	Normalized frequency of chain reversal D
TANS770107	Normalized frequency of left-handed helix
TANS770108	Normalized frequency of zeta R
TANS770109	Normalized frequency of coil
TANS770110	Normalized frequency of chain reversal

Feature	Descriptor
VASM830101	Relative population of conformational state A
VASM830102	Relative population of conformational state C
VASM830103	Relative population of conformational state E
VELV850101	Electron-ion interaction potential
VENT840101	Bitterness
VHEG790101	Transfer free energy to lipophilic phase
WARP780101	Average interactions per side chain atom
WEBA780101	RF value in high salt chromatography
WERD780101	Propensity to be buried inside
WERD780102	Free energy change of epsilon(i) to epsilon(ex)
WERD780103	Free energy change of alpha(Ri) to alpha(Rh)
WERD780104	Free energy change of epsilon(i) to alpha(Rh)
WOEC730101	Polar requirement
WOLR810101	Hydration potential
WOLS870101	Principal property value z1
WOLS870102	Principal property value z2
WOLS870103	Principal property value z3
YUTK870101	Unfolding Gibbs energy in water, pH7.0
YUTK870102	Unfolding Gibbs energy in water, pH9.0
YUTK870103	Activation Gibbs energy of unfolding, pH7.0
YUTK870104	Activation Gibbs energy of unfolding, pH9.0
ZASB820101	Dependence of partition coefficient on ionic strength
ZIMJ680101	Hydrophobicity
ZIMJ680102	Bulkiness
ZIMJ680103	Polarity
ZIMJ680104	Isoelectric point
ZIMJ680105	RF rank
AURR980101	Normalized positional residue frequency at helix termini N4'
AURR980102	Normalized positional residue frequency at helix termini N'''
AURR980103	Normalized positional residue frequency at helix termini N''
AURR980104	Normalized positional residue frequency at helix termini N'
AURR980105	Normalized positional residue frequency at helix termini Nc
AURR980106	Normalized positional residue frequency at helix termini N1
AURR980107	Normalized positional residue frequency at helix termini N2
AURR980108	Normalized positional residue frequency at helix termini N3
AURR980109	Normalized positional residue frequency at helix termini N4

Feature	Descriptor
AURR980110	Normalized positional residue frequency at helix termini N5
AURR980111	Normalized positional residue frequency at helix termini C5
AURR980112	Normalized positional residue frequency at helix termini C4
AURR980113	Normalized positional residue frequency at helix termini C3
AURR980114	Normalized positional residue frequency at helix termini C2
AURR980115	Normalized positional residue frequency at helix termini C1
AURR980116	Normalized positional residue frequency at helix termini Cc
AURR980117	Normalized positional residue frequency at helix termini C'
AURR980118	Normalized positional residue frequency at helix termini C''
AURR980119	Normalized positional residue frequency at helix termini C'''
AURR980120	Normalized positional residue frequency at helix termini C4'
ONEK900101	Delta G values for the peptides extrapolated to 0 M urea
ONEK900102	Helix formation parameters (delta delta G)
VINM940101	Normalized flexibility parameters (B-values), average
VINM940102	Normalized flexibility parameters (B-values) for each residue surrounded by none rigid neighbours
VINM940103	Normalized flexibility parameters (B-values) for each residue surrounded by one rigid neighbours
VINM940104	Normalized flexibility parameters (B-values) for each residue surrounded by two rigid neighbours
MUNV940101	Free energy in alpha-helical conformation
MUNV940102	Free energy in alpha-helical region
MUNV940103	Free energy in beta-strand conformation
MUNV940104	Free energy in beta-strand region
MUNV940105	Free energy in beta-strand region
WIMW960101	Free energies of transfer of AcWL-X-LL peptides from bilayer interface to water
KIMC930101	Thermodynamic beta sheet propensity
MONM990101	Turn propensity scale for transmembrane helices
BLAM930101	Alpha helix propensity of position 44 in T4 lysozyme

Feature	Descriptor
PARS000101	p-Values of mesophilic proteins based on the distributions of B values
PARS000102	p-Values of thermophilic proteins based on the distributions of B values
KUMS000101	Distribution of amino acid residues in the 18 non-redundant families of thermophilic proteins
KUMS000102	Distribution of amino acid residues in the 18 non-redundant families of mesophilic proteins
KUMS000103	Distribution of amino acid residues in the alpha-helices in thermophilic proteins
KUMS000104	Distribution of amino acid residues in the alpha-helices in mesophilic proteins
TAKK010101	Side-chain contribution to protein stability (kJ/mol)
FODM020101	Propensity of amino acids within pi-helices
NADH010101	Hydropathy scale based on self-information values in the two-state model (5% accessibility)
NADH010102	Hydropathy scale based on self-information values in the two-state model (9% accessibility)
NADH010103	Hydropathy scale based on self-information values in the two-state model (16% accessibility)
NADH010104	Hydropathy scale based on self-information values in the two-state model (20% accessibility)
NADH010105	Hydropathy scale based on self-information values in the two-state model (25% accessibility)
NADH010106	Hydropathy scale based on self-information values in the two-state model (36% accessibility)
NADH010107	Hydropathy scale based on self-information values in the two-state model (50% accessibility)
MONM990201	Averaged turn propensities in a transmembrane helix
KOEP990101	Alpha-helix propensity derived from designed sequences
KOEP990102	Beta-sheet propensity derived from designed sequences
CEDJ970101	Composition of amino acids in extracellular proteins (percent)
CEDJ970102	Composition of amino acids in anchored proteins (percent)
CEDJ970103	Composition of amino acids in membrane proteins (percent)
CEDJ970104	Composition of amino acids in intracellular proteins (percent)
CEDJ970105	Composition of amino acids in nuclear proteins (percent)

Feature	Descriptor
FUKS010101	Surface composition of amino acids in intracellular proteins of thermophiles (percent)
FUKS010102	Surface composition of amino acids in intracellular proteins of mesophiles (percent)
FUKS010103	Surface composition of amino acids in extracellular proteins of mesophiles (percent)
FUKS010104	Surface composition of amino acids in nuclear proteins (percent)
FUKS010105	Interior composition of amino acids in intracellular proteins of thermophiles (percent)
FUKS010106	Interior composition of amino acids in intracellular proteins of mesophiles (percent)
FUKS010107	Interior composition of amino acids in extracellular proteins of mesophiles (percent)
FUKS010108	Interior composition of amino acids in nuclear proteins (percent)
FUKS010109	Entire chain composition of amino acids in intracellular proteins of thermophiles (percent)
FUKS010110	Entire chain composition of amino acids in intracellular proteins of mesophiles (percent)
FUKS010111	Entire chain composition of amino acids in extracellular proteins of mesophiles (percent)
FUKS010112	Entire chain composition of amino acids in nuclear proteins (percent)
MITSO20101	Amphiphilicity index
TSAJ990101	Volumes including the crystallographic waters using the ProtOr
TSAJ990102	Volumes not including the crystallographic waters using the ProtOr
COSI940101	Electron-ion interaction potential values
PONP930101	Hydrophobicity scales
WILM950101	Hydrophobicity coefficient in RP-HPLC, C18 with 0.1%TFA/MeCN/H ₂ O
WILM950102	Hydrophobicity coefficient in RP-HPLC, C8 with 0.1%TFA/MeCN/H ₂ O
WILM950103	Hydrophobicity coefficient in RP-HPLC, C4 with 0.1%TFA/MeCN/H ₂ O
WILM950104	Hydrophobicity coefficient in RP-HPLC, C18 with 0.1%TFA/2-PrOH/MeCN/H ₂ O
KUHL950101	Hydrophilicity scale
GUOD860101	Retention coefficient at pH 2
JURD980101	Modified Kyte-Doolittle hydrophobicity scale

Feature	Descriptor
BASU050101	Interactivity scale obtained from the contact matrix
BASU050102	Interactivity scale obtained by maximizing the mean of correlation coefficient over single-domain globular proteins
BASU050103	Interactivity scale obtained by maximizing the mean of correlation coefficient over pairs of sequences sharing the TIM barrel fold
SUYM030101	Linker propensity index
PUNT030101	Knowledge-based membrane-propensity scale from 1D Helix in MPtopo databases
PUNT030102	Knowledge-based membrane-propensity scale from 3D Helix in MPtopo databases
GEOR030101	Linker propensity from all dataset
GEOR030102	Linker propensity from 1-linker dataset
GEOR030103	Linker propensity from 2-linker dataset
GEOR030104	Linker propensity from 3-linker dataset
GEOR030105	Linker propensity from small dataset (linker length is less than six residues)
GEOR030106	Linker propensity from medium dataset (linker length is between six and 14 residues)
GEOR030107	Linker propensity from long dataset (linker length is greater than 14 residues)
GEOR030108	Linker propensity from helical (annotated by DSSP) dataset
GEOR030109	Linker propensity from non-helical (annotated by DSSP) dataset
ZHOH040101	The stability scale from the knowledge-based atom-atom potential
ZHOH040102	The relative stability scale extracted from mutation experiments
ZHOH040103	Buriability
BAEK050101	Linker index
HARY940101	Mean volumes of residues buried in protein interiors
PONJ960101	Average volumes of residues
DIGM050101	Hydrostatic pressure asymmetry index, PAI
WOLR790101	Hydrophobicity index
OLSK800101	Average internal preferences
KIDA850101	Hydrophobicity-related index
GUYH850102	Apparent partition energies calculated from Wertz-Scheraga index
GUYH850103	Apparent partition energies calculated from Robson-Osguthorpe index
) GUYH850104	Apparent partition energies calculated from Janin index

Feature	Descriptor
GUYH850105	Apparent partition energies calculated from Chothia index
JACR890101	Weights from the IFH scale
COWR900101	Hydrophobicity index, 3.0 pH
BLAS910101	Scaled side chain hydrophobicity values
CASG920101	Hydrophobicity scale from native protein structures
CORJ870101	NNEIG index
CORJ870102	SWEIG index
CORJ870103	PRIFT index
CORJ870104	PRILS index
CORJ870105	ALTFT index
CORJ870106	ALTLS index
CORJ870107	TOTFT index
CORJ870108	TOTLS index
MIYS990101	Relative partition energies derived by the Bethe approximation
MIYS990102	Optimized relative partition energies - method A
MIYS990103	Optimized relative partition energies - method B
MIYS990104	Optimized relative partition energies - method C
MIYS990105	Optimized relative partition energies - method D
ENGD860101	Hydrophobicity index
FASG890101	Hydrophobicity index
KARS160101	Number of vertices (order of the graph)
KARS160102	Number of edges (size of the graph)
KARS160103	Total weighted degree of the graph (obtained by adding all the weights of all the vertices)
KARS160104	Weighted domination number
KARS160105	Average eccentricity
KARS160106	Radius (minimum eccentricity)
KARS160107	Diameter (maximum eccentricity)
KARS160108	Average weighted degree (total degree, divided by the number of vertices)
KARS160109	Maximum eigenvalue of the weighted Laplacian matrix of the graph
KARS160110	Minimum eigenvalue of the weighted Laplacian matrix of the graph
KARS160111	Average eigenvalue of the Laplacian matrix of the the graph
KARS160112	Second smallest eigenvalue of the Laplacian matrix of the graph
KARS160113	Weighted domination number using the atomic number

Feature	Descriptor
KARS160114	Average weighted eccentricity based on the the atomic number
KARS160115	Weighted radius based on the atomic number (minimum eccentricity)
KARS160116	Weighted diameter based on the atomic number (maximum eccentricity)
KARS160117	Total weighted atomic number of the graph (obtained by summing all the atomic number of each of the vertices in the graph)
KARS160118	Average weighted atomic number or degree based on atomic number in the graph
KARS160119	Weighted maximum eigenvalue based on the atomic numbers
KARS160120	Weighted minimum eigenvalue based on the atomic numbers
KARS160121	Weighted average eigenvalue based on the atomic numbers
KARS160122	Weighted second smallest eigenvalue of the weighted Laplacian matrix